View metadata, citation and similar papers at core.ac.uk
brought to you by CORE
provided by Juelich Shared Electronic Resources

Cite this: *Soft Matter*, 2011, **7**, 11169

www.rsc.org/softmatter

**PAPER**

# Structure and dynamics of polymer rings by neutron scattering: breakdown of the Rouse model

**Ana R. Brás,*[a] Rossana Pasquino,[c] Thanasis Koukoulas,[ef] Georgia Tsolou,[ef] Olaf Holderer,[b] Aurel Radulescu,[b] Jürgen Allgaier,[a] Vlasis G. Mavrantzas,[ef] Wim Pyckhout-Hintzen,[a] Andreas Wischnewski,[a] Dimitris Vlassopoulos[cd] and Dieter Richter[a]**

***Received 4th July 2011, Accepted 8th September 2011***
**DOI: 10.1039/c1sm06257c**

We present a static and quasi-elastic neutron scattering study on both the structure and dynamics of a ring polymer in a ring and linear polymer melt, respectively. In the first case, the ring structure proved to be significantly more compact compared to the linear chain with the same molecular weight. In the mixture, the ring molecules swell as was confirmed by small angle neutron scattering (SANS) in accordance with both theory and simulation work. The dynamical behavior of both systems, which for the first time has been explored by neutron spin echo spectroscopy (NSE), shows a surprisingly fast center of mass diffusion as compared to the linear polymer. These results agree qualitatively with the presented atomistic MD simulations. The fast diffusion turned out to be an explicit violation of the Rouse model.

Published on 13 October 2011 on http://pubs.rsc.org | doi:10.1039/C1SM06257C
Downloaded by Forschungszentrum Julich Gmbh on 13/05/2013 07:49:17.

## 1 Introduction

The application and industrial processing of many soft condensed-matter systems strongly depend on their rheological properties that are determined by the interactions and motions of the constituent structural units such as chain molecules, aggregates, colloidal particles, and surfactants. Their understanding is one of the great challenges of basic soft condensed matter science and would facilitate the molecular design of new materials. Among these materials polymers stand out. They display very rich dynamics that is currently described in terms of entropically driven Rouse dynamics and the reptation model involving snakelike motions along a tube formed by the mutually interpenetrating chains.[1] In terms of this model, a theory of viscoelasticity has been developed that describes the main features of polymer melt rheology. Reptation including its limiting processes, such as fluctuations of the chain ends (contour length fluctuations, CLF), as well as constraint release (CR) where tube building chains move away laterally, always involve the chain ends in a decisive way.

Having no ends, ring polymers are topologically different and must lack most of the dynamical processes that govern the dynamics of linear and, in particular, branched polymers and indeed recent rheological results display dramatic differences to those from linear chains.[2–4]

In this work we present a new microscopic approach by a combination of SANS and NSE. Before further investigation of large rings,[5] this study focuses on the Rouse regime of rings, smaller than the linear entanglement molecular weight. In fact, all former experimental work on the dynamics of rings concentrated on macroscopic properties.[4,6–17] Therefore, a microscopic understanding of the underlying dynamical processes, which determine the mechanical and rheological properties, is still missing. NSE allows us to directly access the segmental dynamics of a polymer ring. The present work is the first NSE approach to the relaxation mechanisms in a melt of low molecular weight poly (ethylene oxide) (PEO) rings, sustained by a SANS structural characterization. Very recently pulsed-field-gradient (PFG) nuclear magnetic resonance spectroscopy (NMR) results were published on similar systems focusing on the long range diffusion.[16,17] On the contrary, NSE allows investigation of the dynamics on the sample specific length and time scales. Based on NSE spectroscopy in conjunction with SANS, viscosity measurements and MD simulation, we demonstrate a clear violation of the Rouse model with respect to the ring center of mass diffusion. Additionally, it has been found that no internal modes contribute to the dynamics in our NSE window. This is in

[a]*Jülich Centre for Neutron Science JCNS (JCNS-1) & Institute for Complex Systems (ICS), Forschungszentrum Jülich GmbH, 52425 Jülich, Germany. E-mail: a.bras@fz-juelich.de; Fax: +49-2461-61-2610; Tel: +49-2461-61-5093*
[b]*Jülich Centre for Neutron Science JCNS, Forschungszentrum Jülich GmbH, Outstation at FRM II, Lichtenbergstraße 1, 85747 Garching, Germany*
[c]*FORTH, Institute of Electronic Structure and Laser, Heraklion, Crete, 71110, Greece*
[d]*University of Crete, Department of Materials Science and Technology, Heraklion, 71003, Greece*
[e]*University of Patras, Department of Chemical Engineering, Patras, 26504, Greece*
[f]*FORTH-ICE/HT, Institute of Chemical Engineering and High-Temperature Chemical Processes, Patras, 26504, Greece*

Downloaded by Forschungszentrum Julich Gmbh on 13/05/2013 07:49:17.
Published on 13 October 2011 on http://pubs.rsc.org | doi:10.1039/C1SM06257C

agreement with predictions based on a modified dynamic structure factor for ring polymers.

## 2 Experimental

Cyclic protonated and deuterated PEO were obtained from the linear polyethylene glycols.[18] The isotopic purity of the deuterated polymer was 99.9%. Multiple fractionations allowed us to reduce the linear contamination of the cyclic polymers to about 1%. The content of linear polymer was measured for the protonated material by nuclear magnetic resonance ($^1$H NMR) in deuterated pyridine as solvent.[19] As the deuterated ring was synthesized and purified identically, the same quality can be assumed.

Size exclusion chromatography (SEC) in THF/dimethylacetamide (DMAc) with PEO calibration yielded a polymerization degree for the linear polymers $N = 40.2$ for the d-PEO and $N = 42.3$ for the h-PEO, corresponding to $M_n = 1930$ g mol$^{-1}$ (H-equivalent $M_n = 1770$ g mol$^{-1}$) and $M_n = 1860$ g mol$^{-1}$, respectively. It is assumed that the cyclic polymers have the same molecular weights. From $^1$H NMR, $N = 40.9$ for the cyclic h-PEO was obtained, consistent with the SEC value of the linear. The non-uniformity indices $M_w/M_n$ were lower than 1.04. All blends of protonated and deuterated chains (H/D) were prepared in solution and freeze-dried. The volume fraction, $\Phi_H$, of protonated chains was 5 and 20% in SANS and NSE, respectively. The amount of protonated ring in deuterated linear was the same. Given severe restrictions in sample availability for different experiments, the samples used in the rheological measurements were pure, in the order of 99%. For $M \leq M_e$, the contamination of results due to unlinked linear is expected to be low (R. Pasquino *et al.*, unpublished data). Since the effect on NSE was unknown, there the purity was pushed to 99.9% and verified by NMR. This compared very well with a preliminary LCCC (Liquid Chromatography at Critical Condition) test. In future work, we will report separately on the purity and its effect on the properties of larger PEO ring by the combination of NMR and full LCCC analysis.[4,20,21] The mentioned LCCC test could not detect a trace of linear contaminant at an impurity level of $\approx$1% by NMR.

### 2.1 Neutron scattering

Experiments were performed at the SANS diffractometer KWS2 and the spin-echo spectrometer JNSE@FRM2, Munich. At KWS2 the scattering vector range 0.01 Å$^{-1}$ < $Q$ < 0.4 Å$^{-1}$ was accessed whereas the $Q$-range in JNSE was discretely varied between 0.05 Å$^{-1}$ < $Q$ < 0.2 Å$^{-1}$. The temperature of the measurements was chosen to avoid residual crystallization and varied between 373 K (SANS) and 413 K (NSE). The data can be mutually compared as the chain dimension is virtually $T$ independent.[22]

### 2.2 Rheology

The melt viscosities of both samples were measured in a cone-plate geometry using a strain-controlled ARES-HR rheometer equipped with a force rebalance transducer 100FRTN1 from Rheometric Scientific (TA, USA) with Peltier temperature control. A titanium cone and plate geometry with a diameter of 50 mm and a cone angle of 0.04 rad were used for both the steady and the oscillatory experiments on the linear polymer. For the ring polymer, due to limitations in sample quantity, a cone and plate geometry with a diameter of 25 mm and a cone angle of 0.1 rad were instead used. Temperature was controlled by means of a Peltier element, which keeps variations small (±0.05 °C). Measurements were done from 323 to 363 K. The steady shear viscosities of both samples were measured at different rates and temperatures. Both architectures exhibited Newtonian behavior. Small amplitude oscillatory shear experiments were used to confirm the results *via* the Cox-Merz rule, which gave extra credibility to the quality of the results.[23]

## 3 Results and discussion

### 3.1 Rheology

The shear viscosities are plotted as a function of inverse absolute temperature in Fig. 1.

Each point in this plot represents a mean zero-shear viscosity, averaged over different shear rates in the Newtonian region. The corresponding error bars are smaller than the symbols. The lines in Fig. 1 are best fits to the data using an Arrhenius-type expression for the mean zero-shear viscosities, $\eta = A\exp(E/RT)$ with $T$ the absolute temperature, $R$ the universal gas constant, and $A$ and $E$ the fitting parameters. The parameter $E$ is the activation energy. The fitted values for both samples are shown in Table 1. The results indicate that linear and ring polymers have the same activation energies. This result is consistent with an earlier observation of the same shift factors of entangled linear and ring polymers.[4] The viscosity of the ring melt is a factor of 2 lower compared to the linear chains.

### 3.2 SANS

Fig. 2a) shows the obtained SANS scattering profiles for both the linear and the ring polymer, *i.e.* the differential macroscopic scattering cross section $d\Sigma(Q)/d\Omega$ in absolute units (cm$^{-1}$), further abbreviated as intensity $I(Q)$, *versus* scattering vector $Q$. The form factor for a monodisperse ring polymer of arbitrary molecular weight, as it is the case here, can be described by means of a multivariate Gaussian distribution approach as *e.g.* in ref. 24 and in the discrete representation reads

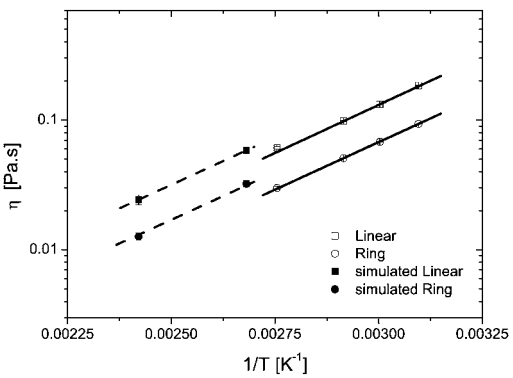


**Fig. 1** Melt viscosity as function of inverse temperature for the linear and ring polymers. For the values obtained by MD simulations, see text.

 This journal is © The Royal Society of Chemistry 2011

Downloaded by Forschungszentrum Julich GmbH on 13/05/2013 07:49:17.
Published on 13 October 2011 on http://pubs.rsc.org | doi:10.1039/C1SM06257C

**Table 1** Parameters for the linear regression (solid lines in Fig. 1) $A_{linear}/A_{ring} = (2.25 \pm 0.17)$

| | $A$ ($10^6$ Pa s) | $E/R$ ($10^{-3}$ K$^{-1}$) |
|---|---|---|
| Linear | 6.3 ± 0.8 | 3.3 ± 0.1 |
| Ring | 2.8 ± 0.2 | 3.36 ± 0.02 |

**Table 2** Parameters extracted from SANS data according to (a) eqn (1) and (b) Beaucage

| | | Ring | Linear | Ring/linear |
|---|---|---|---|---|
| (a) | $R_g$ (Å) | 9.90 ± 0.02 | 14.6 ± 0.07 | 11.13 ± 0.02 |
| (b) | $R_g$ (Å) | 10.08 ± 0.06 | 15.08 ± 0.07 | 11.49 ± 0.07 |
| | $d_f$ | 2.24 ± 0.03 | 1.662 ± 0.004 | 2.24 ± 0.02 |

$$S(Q) = \frac{1}{N^2}\left[N + 2N\sum_{k=1}^{N} F\exp\left\{-\frac{Q^2 l^2 k}{6}F\right\}\right] \quad (1)$$

The ring closure is taken into account by $F = (1 - k/N)$, $k$ being the segment number ($1 < k < N$). For the full description only the number of segments and the average monomer length $l$ is required. The linear Debye analogue is obtained for $F = 1$. The ratio of the squared radii of gyration, $R^2_{g,linear}/R^2_{g,ring} = 2$, is implicit and $R^2_{g,linear}$ is defined as $Nl^2/6$. As the ring was obtained by ring closure of the linear chains its polymerization degree is identical to that of the linear chain. Experimental data for the rings, the ring/linear mixture and the pure linear chains are well described by the discrete summation model using solely the parameter $N$ of the chemical characterization, and varying the statistical monomeric segment length $l$ from which $R_g$ was calculated (see Table 2). The statistical monomeric segment length for this low $M_w$ polymer, found between (5.3 ± 0.1)Å (ring) and (5.4 ± 0.1)Å (linear), as expected, differs by ≈10% from 5.9 Å in the high $M_w$ linear polymer.[25] Both are virtually identical within the accuracy of this experiment. To account for interchain contributions, the random phase approximation was applied.[26] The ring SANS data yield a radius of gyration of $R_g = 9.9$ Å with $M_w = 1706$ g mol$^{-1}$, extracted from $I(Q = 0)$. The linear ring-prepolymer, on the other hand, yields $R_g = 15$ Å, which within experimental uncertainty, confirms the ratio of $\approx\sqrt{2}$ as predicted. Concerning the ring/linear blend a larger $R_g = 11.3$ Å than the pure rings but lower than the linear one was found. This indicates that the cyclic molecules swell as linear chains pervade the volume occupied by them for the volume fraction studied. The experimental swelling is about 12% according to $R_{g,\Phi_R(5\%)}/R_{g,\Phi_R(100\%)} = 1.12$ very close to what was found in the literature for simulated rings with a slightly larger $M_w$ in a blend of linear chains.[27] A quantitative analysis in the $QR_g > 1$ region shows a distinct $Q$ dependence for the different systems following different power laws, $I(Q) \propto Q^{-P}$. For pure ring and linear chains $P = 2.2$ and $P = 1.7$ were found, respectively. For long linear polymers on length scales smaller than $R_g$ the Gaussian chain characteristics correspond to a $Q^{-1/\nu} = Q^{-2}$ dependence with $\nu = 1/2$, *i.e.* the theta state, $\nu$ being the Flory exponent, characterizing the chain statistics and excluded volume effect. Nevertheless, when the chains are too short to explore the Gaussian phase space, an effective slope as in good solvent is observed as we recently reported for short linear PEP[28] despite the Gaussian approximation. For the unentangled linear PEO the unapproximated Debye form factor yields this effective slope naturally. The intermediate $Q$ slope of about $P = 2.2$, which is found for large rings and is the signature of increased correlation, is confirmed here.

The measured $QR_g$-range covering $0.1 < QR_g < 3.5$ prohibits further details. However, in Fig. 2 b), the respective Kratky plot ($IQ^2$ *vs.* $Q$) is instructive. A plateau, which is a signature of a $Q^{-2}$ dependence, is clearly not observed either in the linear case or for the rings and ring/linear cases. In fact, for the ring/linear blend the same power law as for the pure rings is observed. This points to the same structure in both the rings and the ring/linear blend, as further confirmed in the Kratky plot. The development of a shallow peak in the Kratky plot at $Q^* \sim 2/R_g$ is indicative of the compact structure ($P > 2$, $\nu < 1/2$). The missing plateau for the linear chain points to $P < 2$.

The full molecular approach (eqn (1)), can be compared also to recently published work by Beaucage for cyclic structures. His unbiased equation, developed for hierarchical structures, can be viewed as a universal form factor for an arbitrary mass fractal or self-similar object, of which cyclics are prominent examples.[29] The scattering curve from such objects combines two regimes: at low $Q$, the Guinier regime and at high $Q$ the mass-fractal power law regime, *i.e.* $d\Sigma(Q)/d\Omega = G\exp(-Q^2R_g^2/3) + B_f(1/Q^*)^{-d_f}$ with $Q^* = Q/\left[\mathrm{erf}(QKR_g/\sqrt{6})\right]^3$. Here, $d_f$ is the fractal dimension, $K$

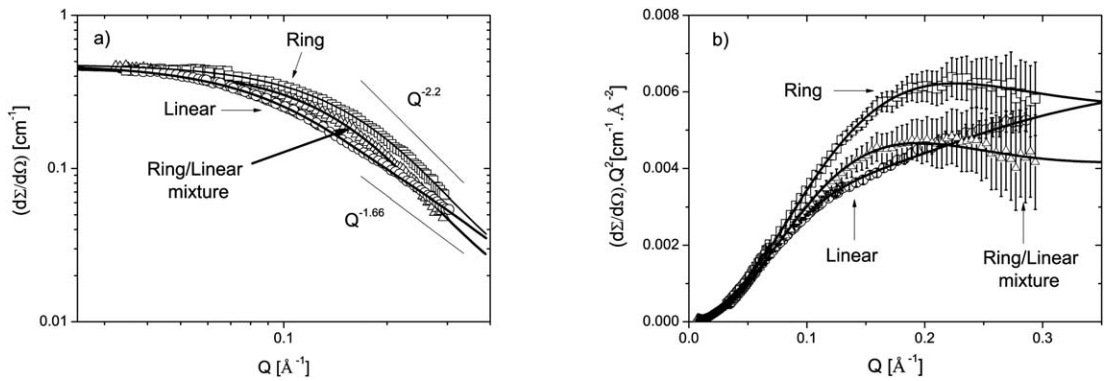


**Fig. 2** a) SANS data on the linear (circles), ring/linear (triangles) and ring (squares) melts. b) The respective Kratky plot for all systems (the symbols are the same as in a)).

Downloaded by Forschungszentrum Julich GmbH on 13/05/2013 07:49:17.
Published on 13 October 2011 on http://pubs.rsc.org | doi:10.1039/C1SM06257C

$\approx 1.06$ an empirical constant and erf is the error function. $G$ and $B_f$ are amplitudes, which for mass fractals can be related to each other by $B_f = d_f G\left(1 - \frac{\ln 2}{\ln z}\right)\Gamma\left(\frac{d_f}{2}\right)/R_g^{d_f}$. Here, $\Gamma$ is the Gamma function and $z$ is the number of Kuhn segments, $z = 24$ as obtained from $R_g$.[22] The fitted parameters are shown in Table 2 as well. By fitting $d_f$, exactly the same power law dependence as in the molecular approach on intermediate length scales is retrieved. The model thus describes the experimental data with comparably good accuracy compared with the molecular approach and indirectly proves that rings are fractal objects. The Beaucage model yields identical results to a recently reported description.[30] However it has been shown recently that beyond our $Q$ range, discrepancies may be expected.

According to Beaucage, the topology of the structures is reflected by the power law found at high $Q$ values, and is quantifiable by $d_f$. The obtained values of $d_f$ clearly show that both the ring and the linear chains have different topologies. Both approaches, eqn (1) and Beaucage, yield the same values for $R_g$. This is not self-evident since a constraint accounting for the closed structure of the ring like in eqn (1) is not present in this simple phenomenological approach. From our experimental results it is concluded that the relation $R^2_{g,linear}/R^2_{g,ring} = 2$ is undoubted and that the cyclic polymer behaves as a fractal object. The different structures, ring *vs.* linear, are expected to affect strongly the dynamics and flow properties. From linear rheology, the extracted viscosity of the ring polymer is a factor of 2 lower than the linear polymer (see Fig. 1).[31,32] This is expected since it has been shown that the calculation of $R_g$ on the one hand and viscosity on the other hand are based on the same matrices and eigenvalues which strongly depend on the architecture. As a consequence, the ratios $R^2_{g,linear}/R^2_{g,ring}$ and $\eta_{linear}/\eta_{ring}$ are the same (see *e.g.* ref. 33 and 34). This result is nicely confirmed in our experiments. Also the activation energies are identical for both ring and linear chains. Therefore the temperature dependence of the segmental friction for the ring and for the linear, can be taken to be the same in good approximation.

### 3.3 NSE

To explore the dynamical properties of the above characterized ring system, for the first time NSE experiments were performed on cyclic polymers. Results obtained for the ring chains are shown in Fig. 3 a). As mentioned above, for short, unentangled polymer chains, one expects Rouse-like behavior that relates to the dynamics of Gaussian chains which is determined by the balance of viscous and entropic forces. The respective single chain dynamic structure factor is then written as:[1,35]

$$S(Q,t) = \frac{1}{N}\sum_{i,j}\exp\left[-Q^2Dt - \frac{Q^2l^2|i-j|}{6} - F - \frac{4Q^2R_G^2}{\pi^2}\sum_p \frac{1}{p^2}E\left[1-\exp(-tp^2/\tau_R)\right]\right] \quad (2)$$

Here, $i$ and $j$ are indices for the segments and $\tau_R$ is the Rouse time of the chain. The first part in the exponential describes the center of mass diffusion with diffusion coefficient $D$, the second term represents the structure of the chain while the third part contains the segmental dynamics, represented by a sum over the Rouse modes $p$ of the polymer chain with a Rouse time, $\tau_R = \frac{\xi N^2 l^2}{3\pi^2 k_B T}$, $\xi$ being the segmental friction. Note that for the ring only even mode numbers contribute due to symmetry.[34] Since the center of mass diffusion is given by $D = \frac{k_B T}{N\xi}$ and $l$ is determined from SANS, the Rouse analysis contains only one free parameter, namely the segmental friction $\xi$. $F$ was defined earlier in connection with eqn (1). The different mode structure for linear and rings is taken into account by $E_{lin} = \cos\left(\frac{p\pi j}{N}\right)\cos\left(\frac{p\pi i}{N}\right)$ and $E_{ring} = \cos\left(\frac{p\pi(j-i)}{N}\right)$, respectively.[34,36] Since the rings are of low molecular weight, the question emerges if the Rouse modes are visible in the probed $Q$ range or not. To clarify this point, a mode contribution analysis using the modified mode structure (eqn (2))[37,34] was performed for both systems. Fig. 3b) presents the mode contribution factors for the linear ($p = 1$, $p = 2$) and for the ring ($p = 2$). Mode contributions with $p = 2$ will show up with measurable intensity for rings of $M_w \geq 5000$ g mol$^{-1}$ for $Q \geq 0.1$ Å$^{-1}$. In the linear case it was already shown earlier that the lowest $Q$ is determined by the center of mass diffusion only, but for the higher $Q$ segmental

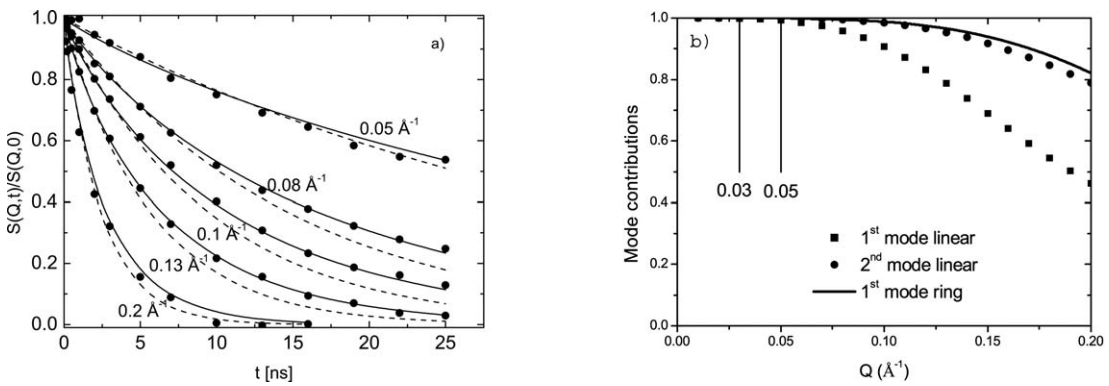


**Fig. 3** a) $S(Q, t)/S(Q, 0)$ *vs.* $t$ for the rings as measured by NSE. Dotted lines show the scattering curves calculated with the Rouse model using the extracted value for $D$ and the solid lines give the fit to the data with a stretched exponential function. b) Contribution factors for the first modes of both the ring and the linear chains to $S(Q, t)/S(Q, 0)$ (see legend in the figure). Note that the first mode for the rings is $p = 2$.

 This journal is © The Royal Society of Chemistry 2011

Downloaded by Forschungszentrum Julich GmbH on 13/05/2013 07:49:17.
Published on 13 October 2011 on http://pubs.rsc.org | doi:10.1039/C1SM06257C

relaxation contributes to $S(Q, t)$. It is obvious that in the ring dynamic structure factor, contrary to the linear chains, only the translational diffusion plays a role in the entire $Q$ and time range probed by the NSE experiment with a minor correction for the two highest $Q$ (see Fig. 3b)). Therefore since in the low $Q$ range no modes contribute to the scattering, it allows us to extract a reliable value for the ring's center of mass diffusion through eqn (2).

Fig. 4 presents the coherent dynamic structure factor of the ring, ring/linear mixture and linear melts for the lowest $Q$ value ($Q = 0.05$ Å$^{-1}$). A fit to the data with the Rouse equation (eqn (2)) is shown by the solid lines. By comparing the scattering curves it is obvious that the rings have significantly faster dynamics, thereby confirming earlier simulation work.[27,34,38,39] For the (more compact) pure rings and the blend with linear, $D = 10.8$ Å$^2$ ns$^{-1}$ and $D = 7.1$ Å$^2$ ns$^{-1}$ are found, respectively. The diffusion coefficient for the linear chains was found to be $D = 5.8$ Å$^2$ ns$^{-1}$ in very good agreement with NSE[35] and PFG-NMR for a very similar PEO,[16,17] the latter on longer time and length scales. The faster diffusion of the ring by a factor of almost 2 is undeniable. Since within the Rouse model $D$ depends only on $\xi$ and $N$ and is therefore independent of architecture, this finding points to a clear violation of the Rouse prediction.

Using the extracted ring value for $D$ one can calculate the scattering curves for all $Q$, using eqn (2), assuming only diffusion which is shown by the dotted curve in Fig. 3a). For $Q \geq 0.08$ Å$^{-1}$ the theoretical curves lie systematically below the experimental data for times longer than 3 ns. The fact that the decay of $S(Q \geq 0.08$ Å$^{-1}$, $t)$ is already overestimated by assuming pure diffusion confirms the results of the presented mode contribution analysis, namely that for the rings no internal modes contribute to the scattering in the entire $Q$ range probed. The deviations from pure diffusion found at higher $Q$, are discussed below. Fig. 5 shows the mean-square displacements *vs.* Fourier time for the lowest $Q$ of the NSE ring data compared to those of the ring/linear mixture and linear chains. These can easily be extracted from the scattering function by $\langle r^2(t)\rangle = \frac{-6}{Q^2}\ln\{S(Q,t)\}$.

While the data of the linear polymer show the well-known subdiffusive behavior with $t^{0.8\pm0.04}$,[40] the ring mean-square displacements are closer to a normal diffusion, with a power of $t^{0.92\pm0.03}$ very similar to simulation results (*e.g.* ref. 38). The

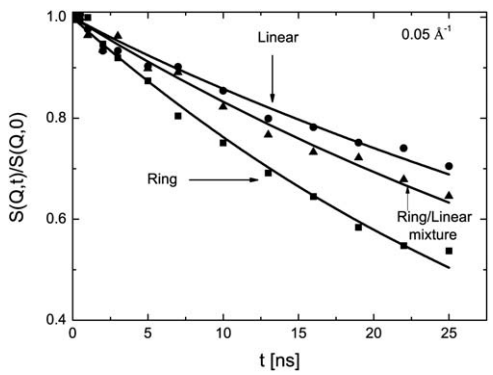


**Fig. 4** $S(Q, t)/S(Q, 0)$ *vs.* $t$ for the ring (squares), ring/linear blend (triangles) and linear (circles) at the lowest $Q$ value ($Q = 0.05$ Å$^{-1}$). The lines are a fit of the data with eqn (2).

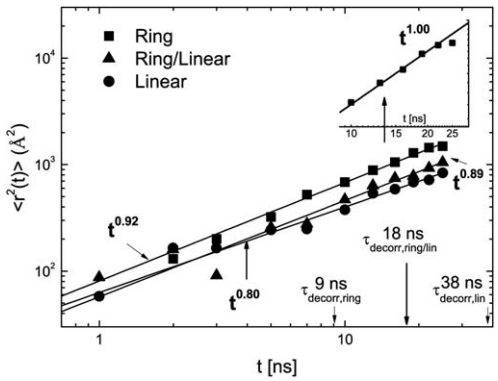


**Fig. 5** Mean-square displacements extracted from $S(Q = 0.05$ Å$^{-1}$, $t)$ for the ring, linear and ring/linear melts as described in the text. On the right a zoom to the rings mean-square displacement data for $t > 9$ ns is displayed.

ring/linear blend with a power of $t^{0.89\pm0.03}$ is situated between the previous values.

Even fitting the whole $Q$ range gives a very similar slope of $t^{0.9\pm0.03}$ and $t^{0.84\pm0.04}$ for the ring and ring/linear, respectively, as presented in Fig. 6.

The solid lines in Fig. 3a) show a fit with a stretched exponential which gives a perfect description of the NSE data in the entire $Q$ and time range yielding $\beta = 0.9$ with $S(Qt) \propto \exp(-(Q^2Dt)^\beta)$. The fit quality is excellent, but the deviation from a $Q^2$ in the single exponential dependence ($Q^{1.8}$) points to a slightly non-Gaussian behavior.

In fact, in a comprehensive NSE study on the center of mass diffusion of short linear polyethylene chains in melts, the subdiffusive behavior could be successfully modeled by a dynamical correlation between the polymers.[41] Here, an adequate interpolymer potential to describe the cooperative dynamics in the melt was used with a range in the order of $R_g$. As a consequence, at a decorrelation time $\tau_{decorr} = R_g^2/D$ at which the mean-square displacement becomes larger than $R_g$, a transition from subdiffusive to diffusive behavior is predicted. Using the values for $R_g$ and $D$ as determined above, we calculate $\tau_{decorr} = 38$ ns for the linear, $\tau_{decorr} = 18$ ns for the ring/linear and $\tau_{decorr} = 9$ ns for the ring polymers. The transition is therefore out of the time window of our NSE measurement in the first case while for the ring and ring/linear the theory predicts a normal diffusion in the accessible time range. The right inset in Fig. 5 shows that for times higher than $\tau_{decorr} = 9$ ns for the pure rings the data are compatible with a pure diffusion (slope = 1). From the mean-square displacements and decorrelation times, one can estimate that the ring moves over a distance of roughly 5 times its $R_g$ in the NSE time window. Since for the ring/linear mixture the decorrelation time is very close to the maximum Fourier times of the experiment, the same cannot be concluded for this system.

### 3.4 Comparison with molecular dynamics simulations

In addition to the SANS and NSE measurements, the structural and dynamic properties of both the ring and linear melts considered here were studied by atomistic molecular dynamics (MD) simulations using the modified TrAPPE united-atom (UA) force-field proposed by Fischer *et al.*[42,43] The corresponding

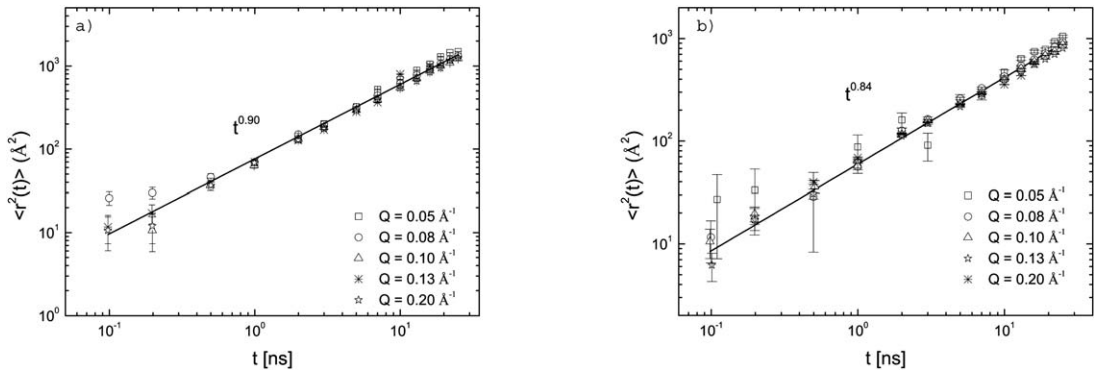


**Fig. 6** The mean-square displacements extracted from all studied $Q$ values for the a) ring and b) ring/linear melts.

Published on 13 October 2011 on http://pubs.rsc.org | doi:10.1039/C1SM06257C
Downloaded by Forschungszentrum Julich Gmbh on 13/05/2013 07:49:17.

potential functions include bond-stretching, bond-bending, torsional, Lennard-Jones and electrostatic interactions. The MD simulations were executed in the NPT statistical ensemble at two different temperatures ($T$ = 413 K and $T$ = 373 K) and at a pressure $P$ = 1 atm, using the GROMACS simulation package.[44] The initial configuration (corresponding to a monodisperse PEO melt with $M_w$ as given above in the experimental) was created using the Materials Studio software package[45] followed by a potential energy minimization procedure and exhaustive pre-equilibration *via* a long NVT MD simulation run at 450 K, at a density value close to the experimental one at this temperature. The two systems simulated consisted of 125 linear PEO chains and PEO rings, respectively. Temperature and pressure were maintained at their prescribed values using a Nosé-Hoover thermostat-barostat.[46–48] The equations of motion were integrated using a single time step MD algorithm equal to 2 fs. For both systems (ring and linear), very long MD trajectories accumulated at both temperatures (up to 300 ns in the case of the lower temperature) to reduce the statistical uncertainty of the configurational averages for the properties of interest. Typical simulation results for the system, *i.e.* longest relaxation time, density, chain dimensions, chain self diffusion coefficient, and the zero shear rate viscosity, are reported in Table 3. They are all in qualitative and in some cases excellent quantitative agreement with the experimentally measured values. The simulation predictions support the experimental findings that: a) the viscosity of the ring polymer is by a factor of 2 lower than that of the linear melt at the same density, and b) ring chains diffuse faster than linear chains (here by approximately 40%). This is a confirmation of the experimental results pointing to a violation of the Rouse model. The simulation predictions for the zero-shear rate viscosity are in excellent quantitative agreement with the measured viscosities for both systems. Moreover the factor of 2 found between the ring and linear viscosities is practically the same in the simulated case. This is nicely shown in Fig. 1 where the two sets of data are perfectly consistent. It is noteworthy that the simulated and experimental activation energies are virtually identical. Besides the confidence in the analysis, these results are also suggestive of the reduced effect of linear contaminants (in small amounts not exceeding $\approx$1%) on ring dynamics for low molecular weights, as compared to large, entangled ones. This will be discussed in much more detail in forthcoming publications. The viscosities were obtained using the longest chain relaxation times ($\tau_{1,L}$, $\tau_{2,R}$) as directly calculated from the MD runs, in the Rouse equations $\eta_{0,R} = (\Pi^2\rho RT/6)\tau_{2,R}$ and $\eta_{0,L} = (\Pi^2\rho RT/6)\tau_{1,L}$.

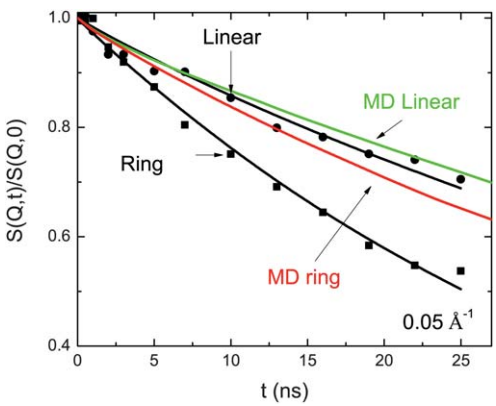


**Fig. 7** Comparison of the normalized dynamic structure factor $S(Q, t)$ *vs.* $t$ for the ring (red line) and linear (green line) melts at the lowest $Q$ value ($Q$ = 0.05 Å$^{-1}$) from MD simulations with NSE data (legend as in Fig. 4).

**Table 3** MD predictions for several properties of interest between the simulated linear and ring PEO systems

| System | Linear ($T$ = 413 K) | linear ($T$ = 373 K) | Ring ($T$ = 413 K) | Ring($T$ = 373 K) |
|---|---|---|---|---|
| $\tau_{1,L}$ (ns) | 8.6 ± 0.2 | 22.0 ± 0.5 | 2.2 ± 0.2 | 6.0 ± 0.2 |
| $\tau_{2,R}$ (ns) | | | | |
| density $\rho$ (g cm$^{-3}$) | 1.000 | 1.040 | 1.015 | 1.055 |
| $<R_g^2>_L$, $<R_g^2>_R$ (Å$^2$) | 235 ± 10 | 240 ± 10 | 110 ± 10 | 115 ± 10 |
| $D$ (Å$^2$ ns$^{-1}$) | 5.4 ± 1.5 | 2.0 ± 0.7 | 7.1 ± 2.6 | 2.5 ± 0.9 |
| $\eta_0$ (Pa s) | (24.3 ± 1.5) × 10$^{-3}$ | (58.3 ± 2.2) × 10$^{-3}$ | (12.6 ± 0.8) × 10$^{-3}$ | (32.2 ± 1.8) × 10$^{-3}$ |


This journal is © The Royal Society of Chemistry 2011

Published on 13 October 2011 on http://pubs.rsc.org | doi:10.1039/C1SM06257C
Downloaded by Forschungszentrum Julich Gmbh on 13/05/2013 07:49:17.

In Fig. 7 the MD predictions for the coherent dynamic structure factor $S(Q, t)/S(Q, 0)$ of both the ring and linear melts are presented for $Q = 0.05$ Å$^{-1}$ and compared with the experimentally measured data for the same $Q$ value. For the linear system very good quantitative agreement is found. Moreover the experimentally significant faster dynamics of the rings is confirmed qualitatively. This validates the atomistic simulations studies presented here.

## 4 Conclusion

Summarizing the NSE results we have found i) the diffusion of the Rouse ring is almost a factor of 2 faster compared to the linear reference with identical molecular weight, ii) the dynamic structure factor for the ring is not affected by internal modes in the accessible time and $Q$ window, iii) in contrast to the linear chains, the ring data show less subdiffusive behavior in the entire Fourier time range and are even compatible with pure diffusion at longer times in agreement with the prediction of a recent approach to the dynamic correlation of polymers in the melt.[41] Concerning the ring/linear mixture, the diffusion coefficient is closer to the linear. The same holds for the subdiffusive behavior. At longer times pure diffusive behaviour is found for the rings, as anticipated.

While the smaller $R_g$ and the lower viscosity of the rings are in quantitative agreement with the Rouse theory, the much faster diffusion demonstrates an obvious violation of this model. The center-of-mass diffusion is clearly not solely determined by segmental friction and the number of segments as predicted in the Rouse model. In contrary it shows an unexpected dependency on the architecture. Our finding of a significantly faster diffusion of rings which have the same number of chemically identical segments therefore is in a definite contradiction to the "heat bath" assumption which the Rouse model is based upon. Moreover, the fact that the center-of-mass diffusion of the present ring/linear mixture at $\Phi_{ring} = 20$ lies between the pure ring and the pure linear values seems to reflect the different ring conformations (compact and slightly swollen). This is confirmed by our complementary SANS study, which points to a very compact structure of the pure ring polymer, especially in the present situation of small molecular weight below the linear entanglement limit. This obviously generates at least partly a shielding of the monomers from the heat bath resulting in a smaller friction per monomer compared to the linear chain and the Rouse prediction, respectively.[38] At the same time, the ring/linear mixture with a swollen ring conformation as found by SANS experiences a reduced shielding due to the interpenetrating linear chains with a consequently slower diffusion compared to the pure rings.

A qualitatively similar, but less pronounced, behaviour for $D$ was found by PGF-NMR and the here presented atomistic MD simulations. The present work is the first experimental validation of simulation results on $R_g$, diffusion and mean-square displacement on the segmental length scale. The SANS results using the Beaucage description prove at least similar properties of a ring compared to a fractal object or a lattice animal. Indeed, the lattice animal representation or an analogy to randomly branched structures has been already proposed for larger polymer rings.[4,49] However, our PEO ring with about 24 Kuhn segments is too small to realize such a conformation.[49] In particular our system is not entangled and the picture of lattice animals implies entanglements or at least long-lived obstacles. These, however, are expected to be absent in large ring systems,[34] even for molecular weights far beyond the entanglement molecular weight ($M_e$). A detailed description of the dynamic behaviour of moderately 'entangled' rings, in particular an extensive analysis of the internal mode dynamics, will be matter of a forthcoming study.

The authors thank T. Chang (Pohang University of Science and Technology, South Korea) for the LCCC analysis. The authors acknowledge EU for funding through the ITN-214627 (DYNACOP). ARB and RP acknowledge DYNACOP for a post-doc grant.

## References

1 M. Doi and S. F. Edwards, *The Theory of Polymer Dynamics*, Clarendon, Oxford, 1986.
2 T. McLeish, *Science*, 2002, **297**, 2005.
3 T. McLeish, *Nat. Mater.*, 2008, **7**, 933.
4 M. Kapnistos, M. Lang, D. Vlassopoulos, W. Pyckhout-Hintzen, D. Richter, D. Cho, T. Chang and M. Rubinstein, *Nat. Mater.*, 2008, **7**, 997–1002.
5 V. Arrighi, S. Gagliardi, A. C. Dagger, J. A. Semlyen, J. S. Higgins and M. J. Shenton, *Macromolecules*, 2004, **37**, 8057.
6 D. Huang, S. L. Simon and G. B. McKenna, *J. Chem. Phys.*, 2005, **122**, 084907.
7 K. Viras, Z.-G. Yan, C. Price, C. Booth and A. J. Ryan, *Macromolecules*, 1995, **28**, 104–109.
8 J. Cooke, K. Viras, G.-E. Yu, T. Sun, T. Yonemitsu, A. J. Ryan, C. Price and C. Booth, *Macromolecules*, 1998, **31**, 3030–3039.
9 K. U. Kirst, K. Kremer, T. Pakula and J. Hollingshurst, *Colloid Polym. Sci.*, 1994, **272**, 1420–1429.
10 A. A. Goodwin, M. S. Beeverst, S. J. Clarson and J. A. Semlyen, *Polymer*, 1996, **37**, 2603–2607.
11 G. B. McKenna, G. Hadziioannou, P. Lutz, G. Hild, C. Strazielle, C. Straupe, P. Rempp and A. J. Kovacs, *Macromolecules*, 1987, **20**, 498–512.
12 J. Roovers, *Macromolecules*, 1988, **21**, 1517–1521.
13 G. B. McKenna, B. J. Hostetter, N. Hadjichristidis, L. J. Fetters and D. J. Plazek, *Macromolecules*, 1989, **22**, 1834–1852.
14 P. G. Santangelo, C. M. Roland, T. Chang, D. Cho and J. Roovers, *Macromolecules*, 2001, **34**, 9002.
15 P. C. Griffiths, P. Stilbs, G.-E. Yu and C. Booth, *J. Phys. Chem.*, 1995, **99**, 16752–16756.
16 S. Nam, J. Leisen, V. Breedveld and H. W. Beckham, *Polymer*, 2008, **49**, 5467–5473.
17 S. Nam, J. Leisen, V. Breedveld and H. W. Beckham, *Macromolecules*, 2009, **42**, 3121–3128.
18 T. S. Sun, G. R. Yu, C. Price, C. J. and A. J. Ryan, *Polymer*, 1995, **36**, 3775.
19 J. Araki, C. Zhao and K. Ito, *Macromolecules*, 2005, **38**, 7524.
20 H. C. Lee, H. Lee, W. Lee, T. Chang and D. Roovers, *Macromolecules*, 2000, **33**, 8119.
21 H. Pasch and B. Trathnigg, *HPLC of Polymers*, Springer, 1997.
22 J. Kugler, E. W. Fischer, M. Peuscher and C. D. Eisenbach, *Makromol. Chem.*, 1983, **184**, 2325–2334.
23 W. W. Graessley, *Polymeric Liquids & Networks Dynamics and Rheology*, Taylor & Francis Group, London and New York, 2008.
24 B. Hammouda, *Adv. Polym. Sci.*, 1993, **106**, 87.
25 L. Fetters, D. Lohse, D. Richter, T. Witten and A. Zirkel, *Macromolecules*, 1994, **27**, 4639.
26 P. G. De Gennes, *J. Chem. Phys.*, 1971, **55**, 572–579.
27 B. V. S. Iyer, A. K. Lele and S. Shanbhag, *Macromolecules*, 2007, **40**, 5995.
28 K. Nusser, S. Neueder, G. J. Schneider, M. Meyer, W. Pyckhout-Hintzen, L. Willner, A. Radulescu and D. Richter, *Macromolecules*, 2010, **43**, 9837.
29 G. Beaucage and A. S. Kulkarni, *Macromolecules*, 2010, **43**, 532–537.

View Article Online

30 B. Hammouda, *J. Appl. Crystallogr.*, 2010, **43**, 1474.
31 H. A. Kramers, *J. Chem. Phys.*, 1946, **14**, 415.
32 J. Semlyen, *Cyclic Polymers*, Kluwer Academic Publishers, Netherlands, 2000.
33 W. W. Graessley, *J. Polym. Sci., Polym. Phys. Ed.*, 1980, **18**, 27.
34 G. Tsolou, N. Stratikis, C. Baig, P. S. Stephanou and V. G. Mavrantzas, *Macromolecules*, 2010, **43**, 10692.
35 K. Niedzwiedz, A. Wischnewski, W. Pyckhout-Hintzen, J. Allgaier, D. Richter and A. Faraone, *Macromolecules*, 2008, **41**, 4866–4872.
36 B. Zimm and W. Stockmayer, *J. Chem. Phys.*, 1949, **17**, 1301.
37 D. Richter, L. Willner, A. Zirkel, B. Farago, L. J. Fetters and J. S. Huang, *Macromolecules*, 1994, **27**, 7437–7446.
38 S. Brown and G. Szamel, *J. Chem. Phys.*, 1998, **109**, 6184.
39 K. Hur, R. G. Winkler and D. Y. Yoon, *Macromolecules*, 2006, **39**, 3975.
40 W. Paul, G. D. Smith and D. Y. Yoon, *Macromolecules*, 1997, **30**, 7772–7780.
41 M. Zamponi, A. Wischnewski, M. Monkenbusch, L. Willner, D. Richter, P. Falus, B. Farago and M. G. Guenza, *J. Phys. Chem. B*, 2008, **112**, 16220–16229.
42 J. Fischer, D. Paschek and G. Sadowski, *J. Phys. Chem. B*, 2008, **112**, 2388.
43 J. Fischer, D. Paschek, A. Geiger and G. Sadowski, *J. Phys. Chem. B*, 2008, **112**, 8849.
44 D. van der SpoelE. Lindahl, B. Hess, A. van Buuren, E. Apol, P. Meulenhoff, D. Tieleman, A. SijbersK. Feenstra, R. van DrunenH. Berendsen, *Gromacs User Manual*, 2010, version 4.5.4, http://www.gromacs.org.
45 *Materials Studio*, Accelrys Software Inc., San Diego, USA.
46 S. Nosé, *Mol. Phys.*, 1984, **52**, 255.
47 S. Nosé, *J. Chem. Phys.*, 1984, **81**, 511.
48 W. Hoover, *Phys. Rev. A: At., Mol., Opt. Phys.*, 1985, **31**, 1695.
49 S. P. Obhukov, M. Rubinstein and T. Duke, *Phys. Rev. Lett.*, 1994, **73**, 1263.

Downloaded by Forschungszentrum Julich Gmbh on 13/05/2013 07:49:17.
Published on 13 October 2011 on http://pubs.rsc.org | doi:10.1039/C1SM06257C

 This journal is © The Royal Society of Chemistry 2011